

Force on a body in a continuously stratified fluid. Part 2. Sphere

By EUGENY V. ERMANYUK AND NIKOLAI V. GAVRILOV

Lavrentyev Institute of Hydrodynamics, 630090, Novosibirsk, Russia
ermanyuk@hydro.nsc.ru

(Received 27 February 2002 and in revised form 7 February 2003)

In this paper the experimental study presented in Part 1 is extended to the three-dimensional case. The in-line force coefficients (added mass and damping) of a sphere oscillating horizontally in a uniformly stratified fluid of limited depth and in a smooth pycnocline are evaluated from Fourier-transforms of the experimental records of impulse response functions. The hydrodynamic loads in the three- and two-dimensional cases are shown to be essentially different, notably in the low-frequency limit, where the damping in the three-dimensional case is zero, while in the two-dimensional case it is maximized due to phenomena akin to blocking. The generalization of the experimental results for affinely similar geometries is discussed. It is found that, as the characteristic vertical extent of stratification decreases, the mean power of internal waves radiated by the oscillating sphere reduces and the maximum of the frequency spectrum of wave power shifts toward lower frequency, which is qualitatively similar to the effects observed in the two-dimensional case. Physically, horizontal stratified waveguides act as low-pass filters since internal waves with nearly vertical group-velocity vector cannot be effectively radiated from oscillating bodies.

1. Introduction

The hydrodynamic loads acting on a circular cylinder oscillating horizontally in a uniformly stratified fluid of limited depth and in a continuously stratified fluid with a smooth pycnocline have been studied experimentally in Part 1 (Ermanyuk & Gavrilov (2002)). In addition to the experimental data, Part 1 presents a literature survey and a brief discussion of some theoretical aspects of the problem.

In Part 2, the present paper, we focus our attention on the three-dimensional problem and investigate experimentally the force coefficients of a horizontally oscillating sphere for the same types of stratification as in Part 1. The experimental results in two- and three-dimensional problems are discussed in the context of the theory of affine similitude described in Ermanyuk (2002). The application of the theory is most straightforward in the case of a uniformly stratified fluid of infinite extent, where an expression for the force coefficients can be obtained, in elliptic problems, by the change of variables in the known solutions for added masses of affinely similar bodies oscillating in a homogeneous fluid (see Korotkin 1986 for a textbook on added masses), and, in hyperbolic problems, by construction of the appropriate analytic continuation. As particular cases, one can obtain the expressions for the hydrodynamic loads, which have been found by alternative approaches in Lai & Lee (1981), Voisin (2003*a, b*) and Hurley (1997) for some bodies of simple geometry (spheroids, spheres, circular and elliptic cylinders).

In the case of a uniformly stratified fluid of finite depth, a properly formulated rule of affine similitude can be used for generalization of experimental data for the affinely similar experimental geometries. Also, one can draw some qualitative conclusions for stratification with a pycnocline. In this connection, investigation of the low-frequency limit for the force coefficients together with some consequences of the Kramers–Kronig relations is of particular interest (see Part 1 and related work Kotik & Mangulis 1962; Wehausen 1971; Landau & Lifshitz 1980). Note that the low-frequency limit for the oscillatory motion of a body in a continuously stratified fluid is physically similar to the low-velocity limit for the motion with uniform velocity. In the latter case, for the horizontal motion, the difference between the two- and three-dimensional problems is manifested by the presence or absence of blocking upstream of a body. In relation to this topic, the work by Vladimirov & Il'in (1990) on the low-velocity limit of hydrodynamic loads in a uniformly stratified fluid presents the concept, which is akin to the one used in the present paper. General discussions on the blocking phenomena can be found for example in Turner (1973) and Baines (1995).

Section 2 of this paper presents a brief theoretical summary. The description of the experimental installation and techniques is given in §3. The results of experiments with a sphere are described in §4, which also presents a discussion of the main effects observed in two- and three-dimensional problems. Concluding remarks concerning the effects of the body geometry, the type of stratification and the direction of oscillations are drawn in §5.

2. Theoretical preliminaries

Let us consider harmonic oscillations of a body with frequency ω in an inviscid uniformly stratified Boussinesq fluid with constant Brunt–Väisälä frequency $N(x_3) = [(-g/\rho) d\rho/dx_3]^{1/2}$, where $\rho(x_3)$ is the density distribution over the vertical coordinate of the Cartesian coordinate system (x_1, x_2, x_3) , and g is the acceleration due to gravity. The fluid domain is confined between two horizontal rigid planes located at $x_3 = \pm H/2$, where H is the total fluid depth.

As it is shown in Ermanyuk (2002), the added-mass coefficients $K_{ij}^{(1)}$ of a body oscillating with frequency $\Omega = \omega/N > 1$ in uniformly stratified fluid of infinite extent ($H \rightarrow \infty$) are related to the added-mass coefficients $K_{ij}^{(2)}$ of a fictitious affinely similar body oscillating in a homogeneous fluid so that

$$K_{ij}^{(1)} = K_{ij}^{(2)} a_i a_j, \quad (2.1)$$

with $a_i = (1, 1, \alpha)$, $K_{ij}^{(1)} = m_{ij}^{(1)}/\rho_c W^{(1)}$, $K_{ij}^{(2)} = m_{ij}^{(2)}/\rho_c W^{(2)}$, where $\alpha = (\Omega^2 - 1)^{1/2}/\Omega$; ρ_c is the reference density at the depth corresponding to the body centre; $m_{ij}^{(1)}$ and $m_{ij}^{(2)}$, $W^{(1)}$ and $W^{(2)}$ are the added masses and volumes of initial and fictitious bodies, respectively. The fictitious body is obtained by compressing the initial body in the vertical direction by a factor α . Relation (2.1) has been obtained in Ermanyuk (2002) by considering the integrals of pressure over the body surface and the control surface surrounding the body, and applying the Gauss theorem to the fluid volume between these surfaces. The control surface can be a material surface that undergoes the same affine transformation as the body surface. In this case, relation (2.1) is valid since the conversion factors relating surface integrals over initial and fictitious bodies as well as over initial and transformed control surfaces are the same. However, one should keep in mind that in the hyperbolic problem ($\Omega < 1$) the control surface cannot be a closed surface. There must be a possibility for radiation of internal-wave energy to infinity. In the present paper we consider a body oscillating between rigid horizontal planes

and the latter requirement is fulfilled. Formula (2.1) relates the added-mass coefficients $K_{ij}^{(1)}$ of a body oscillating in a uniformly stratified fluid of limited depth H and the added-mass coefficients $K_{ij}^{(2)}$ of the fictitious body oscillating in a homogeneous fluid of depth αH . For simplicity we assume that the centres of the original and fictitious bodies are located at the depths $H/2$ and $\alpha H/2$, respectively. Now let us suppose that, for a certain family of bodies oscillating in a homogeneous fluid between two horizontal parallel rigid planes, we know the functions representing the dependence of the added-mass coefficients on non-dimensional geometrical parameters

$$K_{ij}^{(2)} = f_{ij}(e, q, h) \quad (2.2)$$

where $e = b_2/b_1$ and $q = b_3/b_1$ are the relations between the characteristic dimensions b_1, b_2, b_3 of the bodies in the directions x_1, x_2, x_3 , and h is the non-dimensional distance between the planes normalized by the vertical size of the body. Then, $K_{ij}^{(1)}$ of a body with given e_0, q_0 and h_0 can be found as follows:

$$K_{ij}^{(1)}(\Omega) = f_{ij}(e_0, q_0\alpha, h_0)a_i a_j. \quad (2.3)$$

As discussed in Ermanyuk (2002) in context of Hurley (1972), $K_{ij}^{(1)}(\Omega)$ at $\Omega < 1$ can be obtained by analytic continuation in frequency provided the radiation condition formulated in the causal sense holds true, i.e. the internal waves are radiated from the source to infinity and never return back. The analytic continuation for α is $-\imath\eta$, where $\eta = (1 - \Omega^2)^{1/2}/\Omega$ is the real-value parameter. The coefficients a_i should be replaced by $\gamma_i = (1, 1, -\imath\eta)$. Accordingly, expression (2.3) becomes

$$K_{ij}^{(1)}(\Omega) = f_{ij}(e_0, -q_0\imath\eta, h_0)\gamma_i \gamma_j. \quad (2.4)$$

Unfortunately, there are few analytical solutions for the added mass of bodies with arbitrary e and q oscillating in ideal homogeneous fluid between rigid horizontal planes with arbitrary h . The known results are presented in Sedov (1965, Chap. 3, §8), where one can find Sedov's solution for a plate (a body of zero volume), and Gurevich's (1940) solution for a rectangle.

Thus, expressions (2.3) and (2.4) are of easy practical use only for a fluid of infinite extent ($H \rightarrow \infty$), where a multitude of solutions known for ideal homogeneous fluid in terms of $f_{ij}(e, q)$ (see for example Korotkin 1986) can be readily recalculated for ideal uniformly stratified fluid. In particular, for an ellipse we have $f_{11} = q$ (horizontal oscillations) and $f_{33} = 1/q$ (vertical oscillations), which, on substitution in (2.3) and (2.4), yield Hurley's (1997) solution used in Part 1 as the large-depth limit. Since the present paper deals with the case of a sphere, we reproduce below the formulae for the added mass of an oblate spheroid with a vertical axis of revolution oscillating in a homogeneous fluid of infinite extent:

$$K_{11}^{(2)} = K_{22}^{(2)} = \frac{q (\arcsin(1 - q^2)^{1/2} - q(1 - q^2)^{1/2})}{(2 - q^2)(1 - q^2)^{1/2} - q \arcsin(1 - q^2)^{1/2}}, \quad (2.5)$$

$$K_{33}^{(2)} = \frac{1 (1 - q^2)^{1/2} - q \arcsin(1 - q^2)^{1/2}}{q \arcsin(1 - q^2)^{1/2} - q(1 - q^2)^{1/2}}. \quad (2.6)$$

By substituting (2.5) and (2.6) in (2.3) and (2.4) one obtains the expressions for $K_{11}^{(1)}(\Omega) = K_{22}^{(1)}(\Omega)$ and $K_{33}^{(1)}(\Omega)$. The solution for $K_{11}^{(1)}(\Omega)$ has been verified experimentally in Ermanyuk (2002) for a set of spheroids with different length-to-diameter ratios. We should note that for the particular case $q_0 = 1$ (sphere) the solution for $K_{11}^{(1)}(\Omega)$ was first obtained by Voisin (2003a) using a different theoretical approach.

The authors became aware of Voisin's solution in 1998 from a personal communication, which played an essential role in stimulation our research. For a vertically oscillating spheroid, the formula for the added mass $K_{33}^{(1)}(\Omega)$, which follows from (2.3), (2.4) and (2.6), exactly coincides with the solution given by Lai & Lee (1981).

For a set of affinely similar bodies having the same h_0 , e_0 and different q_0 , we can formulate the rule of affine similitude that requires

$$K_{ij}^{(1)}/(a_i a_j) = \text{idem} \quad \text{if} \quad q_0^2(\Omega^2 - 1)/\Omega^2 = q_0^2 \alpha^2 = \text{idem}. \quad (2.7)$$

Thus, the experimental data presented in Part 1 for a certain set of $h_0 = H/D$, where D is the diameter of a circular cylinder, can be easily recalculated for elliptical cylinders with any $q_0 < 1$ for the same set of $h_0 = H/D$, where D should be understood as the vertical axis of an elliptical cross-section. In the same manner, the results presented here for the sphere can be recalculated for oblate spheroids. However, in contrast to the deep-fluid case studied in Ermanyuk (2002), where the rule of affine similitude is experimentally shown to hold with good accuracy, in shallow fluids the role of viscous effects is expected to be more pronounced. As a result, we can expect some departures from rule (2.7) for affinely similar experimental geometries as $h_0 \rightarrow 1$. This issue is addressed in §4.2.3.

For consistency with the notation used in Part 1, we restrict our attention to the horizontal oscillations and use the standard decomposition for the complex force coefficient as is customary in naval hydrodynamics (see for example Newman 1977), i.e. $m_{11}^{(1)}(\omega) = \mu_{11}(\omega) - i\lambda_{11}^w(\omega)/\omega$, where $\mu_{11}(\omega)$ and $\lambda_{11}^w(\omega)$ are the added masses and wave damping coefficients, respectively. The superscript w is introduced in the notation λ_{11}^w to distinguish the damping coefficient in an ideal uniformly stratified fluid, where the internal-wave radiation is the sole mechanism of the energy dissipation, and the experimentally measured total damping coefficient λ_{11} , which contains the contributions due to both internal-wave radiation and viscosity. The corresponding non-dimensional values are defined as

$$\left. \begin{aligned} C_\mu &= \text{Re}[K_{11}^{(1)}] = \mu_{11}/\rho_c W^{(1)}, \\ C_\lambda^w &= \Omega \text{Im}[K_{ij}^{(1)}] = \lambda_{11}^w/\rho_c N W^{(1)}, \\ C_\lambda &= \lambda_{11}/\rho_c N W^{(1)}. \end{aligned} \right\} \quad (2.8)$$

It should be kept in mind that at $\Omega < 1$ the wave radiation produces the dominant contribution to the total damping so that C_λ^w gives a rational estimate for C_λ . At $\Omega > 1$ we have $C_\lambda^w \equiv 0$, and C_λ is governed by viscous effects.

3. Experimental arrangement

The experimental technique used in the present study is similar to the one developed in Ermanyuk (2000) and used in Part 1. In what follows, we restrict our description to the modifications due to the three-dimensional geometry of the present problem. The experiments were carried out in a test tank (0.8 m wide, 0.4 m deep and 1 m long). The experimental installation is shown in figure 1. An acrylic sphere of diameter $D = 6.4$ cm was attached to the lower end of a cross-shaped pendulum having variable restoring moment. The distance between the point of rotation of the pendulum and the centre of the sphere was $l = 60$ cm. The maximum horizontal displacement of the sphere in experimental runs was $0.05D$. The oscillations of the pendulum were induced by dropping a steel ball on a rubber membrane attached to the end of the horizontal bar of the pendulum. The history of damped oscillations measured by an electrolytic

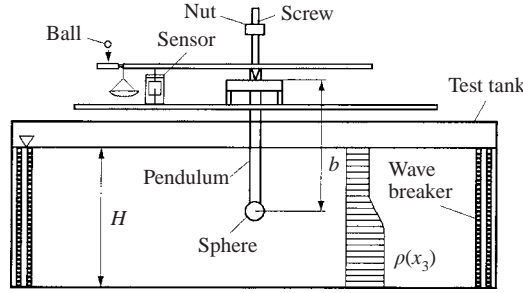


FIGURE 1. Experimental installation.

sensor was sampled at 20 Hz with a 12-bit analog-to-digital converter. To prevent the reflection of internal waves, all vertical walls of the test tank were equipped with the wave-energy absorbers made of a sandwich set of vertical perforated plates.

A weak solution of sugar in water was used to produce a prescribed density distribution. Linear stratification was created by filling the test tank with several layers of fluid. Within two days, the layered structure (the thickness of one layer was about 1.5–2 cm) eventually disappeared due to diffusion. The resulting density distribution was measured by a conductivity probe. These data were used to evaluate the Brunt–Väisälä frequency.

A smooth density profile with a pycnocline was created by filling the test tank with two layers of miscible fluids. In the coordinate system (x_1, x_2, x_3) introduced in §2, with the origin taken at the centre of the sphere submerged to the depth $H/2$, the measured density distribution over depth was fitted the following approximation:

$$\rho(x_3) = \rho_0 \left[1 - \frac{\epsilon}{2} \tanh\left(\frac{2x_3}{\delta}\right) \right], \quad \rho_0 = \frac{\rho_1 + \rho_2}{2}, \quad \epsilon = \frac{\rho_2 - \rho_1}{\rho_1},$$

where δ is the characteristic thickness of the pycnocline, ρ_1 and ρ_2 are the fluid densities in the upper and lower layers, respectively. The experiments were performed at $\epsilon = 0.006$. In Part 1, the effect of variation of ϵ on the force coefficients has been studied in detail. The maximum Brunt–Väisälä frequency in the pycnocline can be estimated as $N_m = (\epsilon g / \delta)^{1/2}$. For the experiments in a pycnocline the non-dimensional damping coefficient is defined by (2.8), with N replaced by N_m .

The technique of the response function analysis used in the present paper is identical to the one described in Part 1. It uses the well-known property of any linear system that its response $\chi(t)$ to a harmonic forcing $f_0(t) = f_0^* \exp(i\omega t)$ is related to the response $r(t)$ to a unit impulse as

$$\chi(t) = f_0^* \exp(i\omega t) R(\omega),$$

where $R(\omega) = R_c(\omega) - iR_s(\omega) = \int_0^\infty r(\tau) \exp(-i\omega\tau) d\tau$.

Substituting $x_1 = \chi$ in the equation of forced horizontal oscillations of a body in frequency domain

$$(M + \mu_{11}(\omega)) \frac{d^2 x_1}{dt^2} + \lambda_{11}(\omega) \frac{dx_1}{dt} + c_{11} x_1 = f_0^* \exp(i\omega t), \quad (3.1)$$

where M is the inherent mechanical inertia of the system and c_{11} is the restoring force coefficient, one can obtain the following formulae for the frequency-dependent added

mass and damping:

$$\mu_{11} = \frac{c_{11}}{\omega^2} \left(1 - \frac{|R(0)|}{|R(\omega)|} \cos(\theta(\omega)) \right) - M, \quad (3.2)$$

$$\lambda_{11} = \frac{c_{11}|R(0)|}{\omega|R(\omega)} \sin(\theta(\omega)), \quad (3.3)$$

where $|R(\omega)| = (R_c^2 + R_s^2)^{1/2}$, $\theta(\omega) = \arcsin(R_s/R_c)$ and $|R(0)|$ denotes $|R(\omega)|$ at zero frequency.

4. Experimental results and discussion

4.1. Homogeneous water

As has already been mentioned in Part 1, the available experimental information on the force coefficients of a body oscillating in a homogeneous fluid is primarily related to the case of relatively high Keulegan–Carpenter and Stokes numbers, with special emphasis on circular cylinders as the main structural elements of marine platforms and rigs. The case of spherical geometry has received little attention. Some experimental information on the inertial and drag force coefficients of a fixed sphere in an oscillatory orbital flow of homogeneous fluid (surface waves) can be found in Iwata & Mizutani (1987) and Iwata, Mizutani & Kasai (1989). An interesting discussion of the role of forces due to acceleration, velocity and history of motion is presented in Odar & Hamilton (1964) and Karanfilian & Kotas (1978) for a sphere oscillating in homogeneous fluid of infinite extent.

Since we are concerned in the present research with the specific case of limited fluid depth, small oscillation amplitudes, and moderate Stokes numbers, i.e. in the range of parameters that has not been studied previously, a series of experiments in homogeneous water has been conducted. The experimental data obtained in homogeneous water can be interpreted in the context of a classic Stokes' asymptotic theory for $a/D \ll 1$ and $\beta = D^2\omega/\nu \gg 1$ (see Stokes 1851; Batchelor 1967, § 5.13; Wang 1968; Landau & Lifshitz 1987, Chap. 2, § 24), where a is the amplitude of oscillations, and ν is the kinematic viscosity. For a sphere oscillating in unbounded viscous fluid this theory yields the following in-line values of added-mass and damping coefficient:

$$\mu = \frac{\pi}{12} \rho D^3, \quad \lambda = 3\pi D \eta (\beta/8)^{1/2}, \quad (4.1)$$

where $\eta = \rho\nu$ is the dynamic viscosity of fluid.

The present experiments were conducted for a set of non-dimensional water depths $H/D = 5.81, 2.11, 1.43, 1.19, 1.063$. It is found that in the studied range of parameters the added-mass coefficient of the sphere depends only on the depth of fluid. The mean measured values are $C_\mu = 0.52, 0.57, 0.64, 0.7, 0.77$, respectively. The scatter of the experimental points about the mean values of C_μ does not exceed $\pm 4\%$. The increase of the added-mass coefficient is notable as H/D approaches 1; however, its overall variation with depth is much smaller than in the two-dimensional case studied in Part 1. It can be shown that, if the added-mass coefficient of a body in homogeneous fluid of infinite extent is $O(1)$, then the leading term of the additive correction due to the presence of the rigid plane boundaries close to the body is $O(\kappa^2)$ and $O(\kappa^3)$ in the two- and three-dimensional cases, respectively, where $\kappa = D/H$. Construction of the solution correct to $O(\kappa^3)$ for a sphere moving near a plane is presented, for example, in Milne-Thomson (1960, see Chap. 16). The procedure can be generalized to

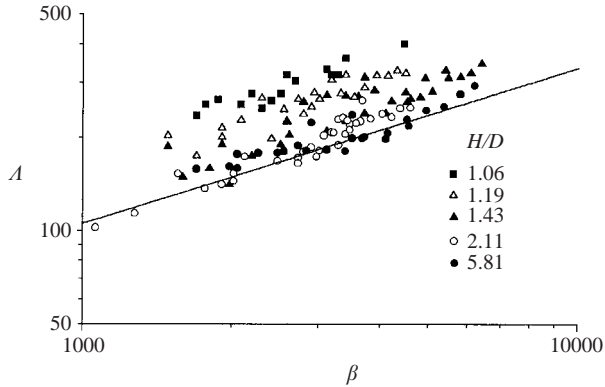


FIGURE 2. Non-dimensional damping Λ vs. Stokes number β for homogeneous fluid of limited depth. Solid line: formula (4.1) for $H/D \rightarrow \infty$.

a two-dimensional case and more complicated geometries as discussed, for example, in Newman (1977, § 4.18) and Sedov (1965, Chap. 3, § 8). Note also that in the limiting case $H/D = 1$ the two-dimensional fluid flow is completely blocked by the cylinder ($\mu \rightarrow \infty$), while in the case of sphere the fluid is free to flow around the body (μ is finite).

The values of the damping coefficient $\Lambda = \lambda/(\eta D)$ versus β for different H/D are plotted in figure 2 on a logarithmic scale. For all values of the fluid depth H/D the law $\Lambda \sim \beta^{1/2}$ is satisfied well. Note that the experimental dependence of Λ on β measured at $H/D = 5.81$ is very close to the theoretical one predicted by (4.1) for homogeneous viscous fluid of infinite extent (solid line in figure 2). To quantify the effect of limited depth we introduce the coefficient $\chi(H/D) = \Lambda(H/D)/\Lambda(\infty)$, where $\Lambda(H/D)$ are experimental values and $\Lambda(\infty)$ is the theoretical dependence for $H/D \rightarrow \infty$. For $H/D = 5.81, 2.11, 1.43, 1.19, 1.063$, the least-squares method yields $\chi(H/D) = 1.05, 1.07, 1.24, 1.43, 1.73$, respectively. In the case of sphere the effect of fluid depth on χ is, quantitatively, less pronounced than in the two-dimensional case (compare with figure 2 of Part 1), where for $H/D = 7.57, 4.32, 3.24, 2.19, 1.65$ we have $\chi(H/D) = 1.15, 1.42, 1.61, 2.34, 3.63$. The experimental data presented in Part 1 and here suggest that $\Lambda(H/D)$ can be estimated using a version of the classic Stokes' approach (see Batchelor 1967, § 5.13; Landau & Lifshitz 1987, Chap. 2, § 24) by evaluating the energy dissipated in oscillatory boundary layers on the body surface and on the boundaries above and below the body.

As in Part 1, to facilitate an explicit quantitative comparison, the results of experiments in homogeneous water are also presented in terms of $C_z(\Omega)$ together with the experimental data obtained in linearly stratified fluid. In this case the normalization of λ_{11} measured in homogeneous water by the wave damping scale $\rho_c N W^{(1)}$ is purely formal.

4.2. Linear stratification

4.2.1. Three-dimensional case

The effect of limited depth for linearly stratified fluid was studied at $H/D = 1.19, 1.43, 2.11, 5.81$. The value of the Brunt–Väisälä frequency in all experimental runs was $N = 1 \text{ rad s}^{-1}$, with accuracy about $\pm 2\%$. The experimental curves $C_\mu(\Omega)$ and $C_\lambda(\Omega)$ are shown in figures 3 and 4, respectively. Solid lines show the theoretical curves obtained from (2.3), (2.4) and (2.5) for a sphere ($q_0 = 1$) oscillating horizontally in a

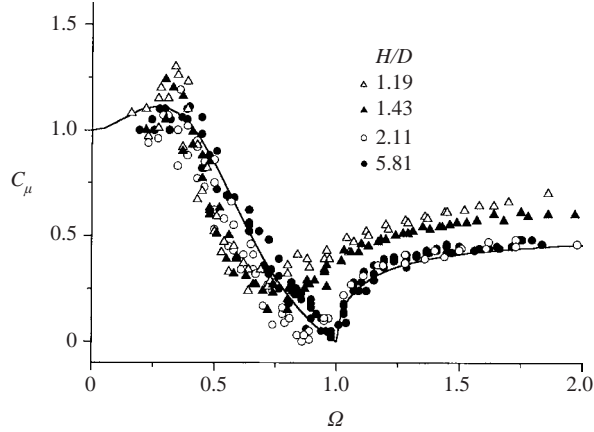


FIGURE 3. Added-mass coefficient C_μ vs. frequency Ω in linearly stratified fluid of limited depth. Solid line: theory for $H/D \rightarrow \infty$.

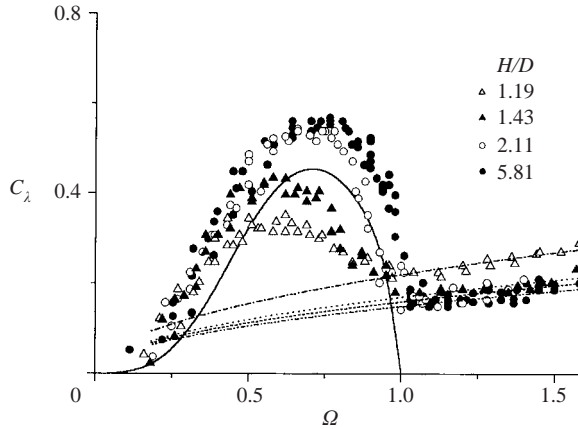


FIGURE 4. Damping coefficient C_λ vs. frequency Ω in linearly stratified fluid of limited depth. Solid line: theory for $H/D \rightarrow \infty$; other lines show experimental data obtained in homogeneous fluid for $H/D = 1.19$ (dash-dot); 1.43 (dot); 2.11 (dash); 5.81 (double dot-dash).

uniformly stratified fluid of infinite extent. The theoretical dependence for the added-mass coefficient (figure 3) is supported well by the experimental data obtained at $H/D = 5.81$, while the measured values of total damping coefficient are systematically higher than the theoretical ones (figure 4). This departure is caused by the additional damping due to viscosity in the real stratified fluid.

In the low-frequency limit ($\Omega \rightarrow 0$) the impermeability condition at the horizontal planes above and below the body is fulfilled automatically since the fluid velocity vector is horizontal. As $\Omega \rightarrow 0$ the three-dimensional problem for horizontal oscillations of a body reduces to a set of two-dimensional Laplace equations with impermeability boundary conditions for each horizontal cross-section of the body. Thus, for any depth of a uniformly stratified fluid and any axisymmetric body with vertical axis of revolution, the low-frequency limit is $C_\mu(0) = 1$. Although the scatter of data at low frequency is considerable, this conclusion agrees well with the data presented in figure 3. Because of the quasi-two-dimensional character of fluid motion at low

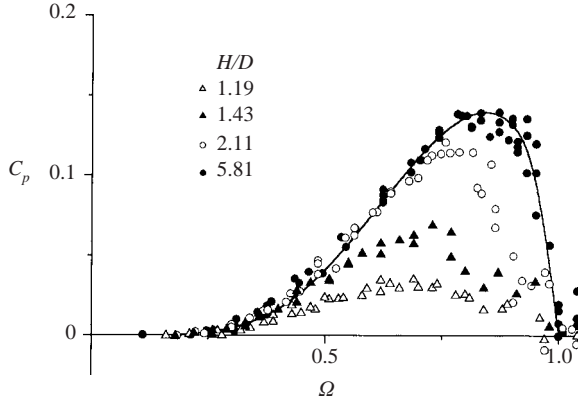


FIGURE 5. Non-dimensional radiated wave power C_p vs. frequency Ω in linearly stratified fluid of limited depth. Solid line: theory for $H/D \rightarrow \infty$.

frequency, we can assume that the curves $C_\mu(\Omega)$ and $C_\lambda(\Omega)$ measured at any depth in uniformly stratified fluid should almost coincide in a certain frequency range close to $\Omega = 0$, which can, indeed, be observed in figures 3 and 4 for $\Omega < 0.3$. As mentioned in Part 1, since in the three-dimensional problem there is no singularity of function $\mu_{11}(\omega) - i\lambda_{11}(\omega)/\omega$ at zero frequency, the integral

$$I = \int_0^\infty [C_\mu(\Omega) - C_\mu(\infty)] d\Omega \quad (4.2)$$

should have zero value for any H/D . This conclusion seems to be consistent with the data shown in figure 3.

To separate the wave and viscous damping in experimental data we use the approach formulated in Part 1. The summary damping coefficient $\lambda_{11}(\omega)$ measured in experiments is schematically represented as a sum of the wave damping $\lambda_{11}^w = C_\lambda^w \rho_c N W^{(1)}$ and viscous damping $\lambda_{11}^v = C_\lambda^v \rho_c D^2 (\omega\nu)^{1/2}$. Furthermore, we assume that $C_\lambda^v = \text{const}$, which, for a given geometry of the problem, has approximately the same value both in stratified and homogeneous fluid (i.e. $C_\lambda^v \approx \Lambda/\beta^{1/2}$). In non-dimensional form, we have

$$C_\lambda(\Omega) = C_\lambda^w(\Omega) + \frac{6}{\pi} \left(\frac{\Omega}{\beta_N} \right)^{1/2} C_\lambda^v, \quad (4.3)$$

where $\beta_N = D^2 N/\nu$ is the ‘internal’ Stokes number (in the experiments with linearly stratified fluid $\beta_N = 3590$). Applying (4.3) to the data presented in figure 4, we can obtain an estimate of the non-dimensional radiated internal-wave power $C_p(\Omega) = C_\lambda^w \Omega^2/2$ for horizontal oscillations of a sphere with unit amplitude. The resulting experimental estimate for $C_p(\Omega)$ is shown in figure 5 together with the theoretical curve recalculated from the curve plotted in figure 4 (solid line). One can see good agreement between the theoretical prediction for $H/D \rightarrow \infty$ and the experimental data for $H/D = 5.81$. In the three-dimensional case, as compared to the two-dimensional one (see figure 4 of Part 1), the frequency range where $C_p(\Omega)$ has significantly higher values is more narrow, being shifted toward the ‘violet’ end of the spectrum. Indeed, at low Ω we have, at leading order, $C_p \sim \Omega^2$ and $C_p \sim \Omega^4$ for two- and three-dimensional problems, respectively. The main effects due to the limited depth, i.e. the ‘red shift’ in the position of the maximum of the radiated wave power and the decrease of its magnitude, are qualitatively the same both in two- and three-dimensional problems.

4.2.2. Two-dimensional case

Some comments should be made on the experimental curves $C_\lambda(\Omega)$ and $C_\mu(\Omega)$ presented in figures 3 and 5 of Part 1. As follows from (2.4), to study the low-frequency behaviour in the two-dimensional problem at $h_0 \rightarrow \infty$, we should consider the limiting value of $C_\lambda^w(\Omega) = \Omega \text{Im}[f_{11}(-iq/\Omega)]$ as $\Omega \rightarrow 0$. For an elliptic cylinder oscillating in unbounded ideal fluid $f_{11} = q$. Hence, for circular cylinder with $q_0 = 1$ we have $C_\lambda^w(0) = 1$. In principle, it can be shown that for a cylinder with vertical size D and cross-sectional area S the low-frequency limit $C_\lambda^w(0) = \pi D^2/4S$, which is related to the fact that as $q \rightarrow \infty$ any two-dimensional body degenerates into a vertical flat plate with the added mass $m_{11}^{(2)} = \pi D^2/4$. In other words, the low-frequency limit for the dimensional damping λ_{11} in two-dimensional problem depends only on the vertical size of an oscillating cylinder ($\lambda_{11} \sim D^2$) and not on the shape of its cross-section. Physically, this corresponds to the effect of blocking in the low-velocity limit for horizontal translational motion with uniform velocity. Note that this analogy can be made explicit by considering complex-valued ω in the function $\exp(i\omega t)$ that expresses the time-dependent part of the main parameters of the present problem. In particular, the motion of a body with velocity $v(t) = \epsilon_0 v_0 \exp(\delta_0 t)$, where $|v_0| = 1$, ϵ_0 and δ_0 are small positive parameters, has been considered in Vladimirov & Il'in (1991), with the special emphasis on the effects that occur in the low-velocity limit.

As already mentioned, the fluid velocity vector as $\Omega \rightarrow 0$ is horizontal, so that any horizontal fluid plane above or below the body can be replaced by a rigid material plane. Thus, we can conclude that for a given body the limiting value $C_\lambda^w(0)$, which is related to the vertical size of the blocked region, is practically independent of the fluid depth H , i.e. $C_\lambda^w(0) \approx \text{const}$ at any H . However, this of necessity implies that for this situation $I \approx \text{const}$ regardless to the actual value of H , since in the two-dimensional case

$$I = -\pi C_\lambda^w(0)/2, \quad (4.4)$$

which can be demonstrated by the residue calculus (see Part 1 for the particular case of Hurley's (1997) solution for a circular cylinder). The above-formulated conjectures agree well with the observed behaviour of experimental curves $C_\lambda(\Omega)$ and $C_\mu(\Omega)$ shown in figures 3 and 5 of Part 1 (it should be kept in mind that $C_\lambda^w(\Omega) \approx C_\lambda(\Omega)$ at $\Omega \rightarrow 0$). We should note that it seems difficult to formulate a simple rule for the limiting value $C_\mu(0)$ at different H/D , since the variation of H/D affects the infinite-frequency limit $C_\mu(\infty)$, which is present in the Kramers–Kronig relations (see Part 1) and in (4.2).

4.2.3. Affine similitude

The rule of affine similitude (2.7) has been verified in Ermanyuk (2002) for large h_0 (in practical terms, for $h_0 \rightarrow \infty$). It was shown that the experimental values of $\text{Re}[K_{11}^{(1)}]$ and $\text{Im}[K_{11}^{(1)}]$ plotted as functions of $q_0^2 \alpha^2$ for spheroids with different q_0 coincide with remarkable accuracy. However, from the data presented in Part 1 and here, we can conclude that the role of viscous effects increases as $h_0 \rightarrow 1$. Therefore, at low h_0 we can expect some departures from (2.7). To clarify this issue we complemented the series of experiments with the sphere by additional experiments with a vertical elongated spheroid having length-to-diameter ratio $L/D = 2 : 1$. The maximum diameter of the spheroid was equal to the diameter of the sphere. The experiments were conducted at constant ratio between the fluid depth H and the vertical size of the bodies (L for the spheroid and D for the sphere), so that in both experimental runs $h_0 = 1.19$. The total measured damping coefficient was decomposed into the wave and viscous components

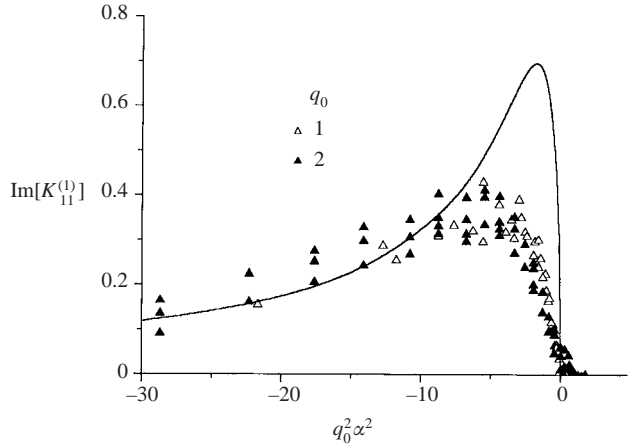


FIGURE 6. Imaginary part of the force coefficient $\text{Im}[K_{11}^{(1)}]$ vs. affine similitude criterion $q_0^2 \alpha^2$ for spheroids with different q_0 in linearly stratified fluid at fixed $h_0 = 1.19$. Solid line: theoretical curve for $h_0 \rightarrow \infty$.

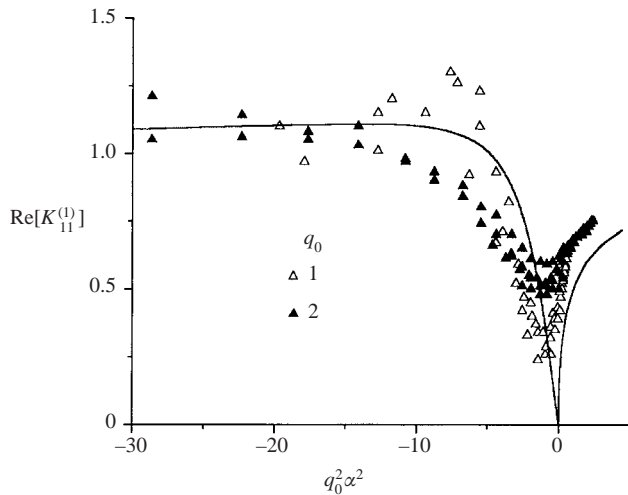


FIGURE 7. Real part of the force coefficient $\text{Re}[K_{11}^{(1)}]$ vs. affine similitude criterion $q_0^2 \alpha^2$ for spheroids with different q_0 in linearly stratified fluid at fixed $h_0 = 1.19$. Solid line: theoretical curve for $h_0 \rightarrow \infty$.

using (4.3), and the final results are plotted as $\text{Im}[K_{11}^{(1)}] = C_\lambda^w / \Omega$ and $\text{Re}[K_{11}^{(1)}] = C_\mu$ versus $q_0^2 \alpha^2$ in figures 6 and 7, respectively. One can see good agreement between the experimental results for the imaginary part of the force coefficient. This, in particular, implies that decomposition (4.3) is physically adequate. For the real part of the force coefficient there is good agreement in the position of the minima for the data obtained at $q_0 = 2$ and $q_0 = 1$. However, there are some quantitative differences in the magnitudes of the real parts of the force coefficients, which can be presumably attributed to viscous effects. For the real part of the force coefficient it seems difficult to formulate a rule for separation of wave and viscous components. One possible reason for the limited accuracy of (2.7) in a stratified fluid of finite depth is the presence of boundary layers on the surface of the oscillating bodies. The boundary-layer

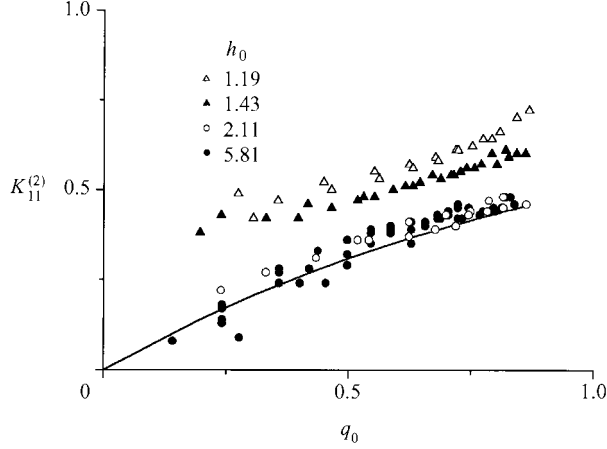


FIGURE 8. Added-mass coefficient $K_{11}^{(2)}$ of oblate spheroids vs. length-to-diameter ratio q_0 in homogeneous fluid with given h_0 (the data are recalculated from figure 3). Solid line: theoretical dependence (2.15) for $h_0 \rightarrow \infty$.

thickness of order $(\nu/\omega)^{1/2}$ is approximately the same for the sphere and the ellipsoid. When $h_0 \rightarrow 1$ a considerable portion of the gap between the ends of the body and the horizontal plane boundaries is occupied by the boundary layers. As result, two experimental systems with the same h_0 are, strictly speaking, not affinely similar, with certain impact on the accuracy of (2.7).

The solid lines in figures 6 and 7 show the universal dependence obtained from (2.5), which is valid for a spheroid with arbitrary q_0 oscillating in a uniformly stratified fluid of infinite extent. Note that for $q_0^2 \alpha^2 < -10$ the experimental points obtained at $h_0 = 1.19$ fall on the universal curve for $h_0 \rightarrow \infty$. In other words, for large q_0 and small Ω the effects of limited depth for a horizontally oscillating body are negligible, as could be expected from general physical reasoning.

Rule (2.7) generalizes the data presented in Part 1 and here for elliptic cylinders and spheroids. In particular, the data from figure 3 obtained at $\Omega > 1$ in the linearly stratified fluid can be recalculated for the case of homogeneous fluid as shown in figure 8, which represents the dependence of the added mass $K_{11}^{(2)}$ of oblate spheroids on the length-to-diameter ratio q_0 at different h_0 . The solid line shows the theoretical dependence $f_{11}(q)$ given by (2.5) for spheroids in homogeneous fluid of infinite extent. At this point it seems pertinent to make a few remarks on a possible approach to the numerical solution of the problem. As has been already mentioned in §2, at $\Omega = 1$ the governing equation of the problem changes its type from elliptic to hyperbolic. Therefore, we can expect that, in general, different numerical methods are effective at $\Omega < 1$ and $\Omega > 1$ (see Sturova 2001). However, the direct solution of the problem at $\Omega > 1$ can be replaced by the solution of the problem for the fictitious affinely similar bodies in homogeneous fluid, which yields dependences similar to those shown in figure 8. Note that the data shown in figure 8 imply that the corresponding numerical calculations should not present significant numerical problems since the functions sought are expected to be reasonably smooth and well-defined. Once the problem is solved for a family of affinely similar bodies in homogeneous fluid, the solution of the original problem at $\Omega > 1$ can be readily obtained from (2.3). Furthermore, the numerical results at each h_0 can be approximated by an analytical function $f_{11}(q)$, which can, in turn, be used for the construction of the analytic continuation according

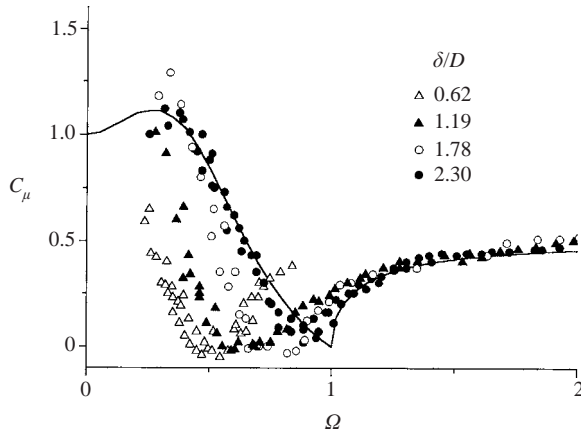


FIGURE 9. Added-mass coefficient C_μ vs. frequency Ω in a pycnocline. Solid line: theory for uniformly stratified fluid of infinite extent.

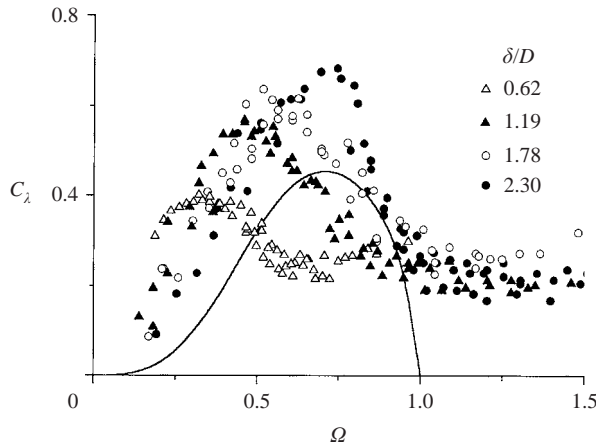


FIGURE 10. Damping coefficient C_λ vs. frequency Ω in a pycnocline. Solid line: theory for uniformly stratified fluid of infinite extent.

to (2.4). For example, one can use spline-interpolation for the points representing $f_{11}(q)$ and construct the analytic continuation by progressing along the spline and replacing q with $-iq_0\eta$.

4.3. Pycnocline

4.3.1. Three-dimensional case

The experiments in the stratified fluid with a pycnocline were carried out at $\epsilon = 0.006$. The total fluid depth in all the cases considered was $H = 28$ cm. The non-dimensional characteristic thickness of the pycnocline varied in the range $0.62 \leq \delta/D \leq 2.3$. The measured values of $C_\mu(\Omega)$ and $C_\lambda(\Omega)$ are presented in figures 9 and 10.

The behaviour of $C_\mu(\Omega)$ in the low-frequency limit can be understood from simple physical reasoning. If the typical vertical length scale of stratification δ is much smaller than the vertical size of the sphere D , the fluid motion at $\Omega \rightarrow 0$ is similar to the motion that occurs in homogeneous fluid almost everywhere except for a thin layer of order δ . Therefore, in the limiting case $\delta/D \rightarrow 0$ we can expect $C_\mu(0) \simeq 0.5$. On the

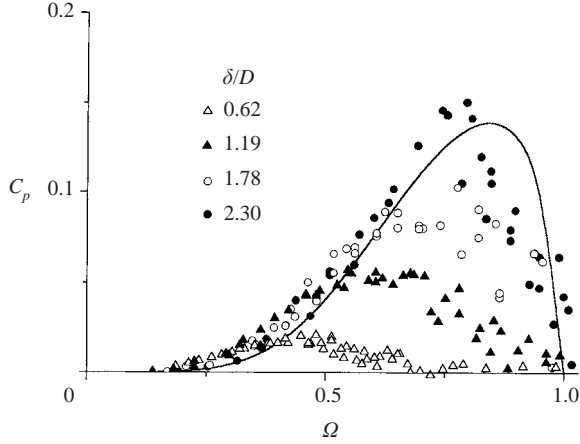


FIGURE 11. Non-dimensional radiated wave power C_p vs. frequency Ω in a pycnocline. Solid line: theory for uniformly stratified fluid of infinite extent.

other hand, for $D \gg \delta$ we can expect $C_\mu(0) = 1$, similar to the case of a uniformly stratified fluid. For the intermediate case $\delta/D = O(1)$, the values of $C_\mu(0)$ fall in the range between 0.5 and unity. Although experimental data at zero frequency could not be obtained because of obvious technical limitations, the behaviour of experimental curves shown in figure 6 seems to agree with the above conjectures.

As $\Omega \rightarrow \infty$, $C_\mu(\infty) = 0.5$ for any δ/D since in experiments with a pycnocline $H \gg D$. Thus, for different δ/D , we have different values of $C_\mu(0)$ and the common value $C_\mu(\infty) = 0.5$. In the uniformly stratified fluid of limited depth the low- and high-frequency behaviour of $C_\mu(\Omega)$ at different H/D is exactly the opposite, as discussed in § 4.2.1, i.e. the values of $C_\mu(\infty)$ are different whereas the value $C_\mu(0) = 1$ is common.

Similarly, there is an important difference between the curves $C_\lambda(\Omega)$ in uniformly stratified fluid and in a pycnocline (compare figures 4 and 10). In the former case, the curves $C_\lambda(\Omega)$ measured at different H/D almost coincide at low Ω . In the latter case, the shape of curves $C_\lambda(\Omega)$ changes with δ/D in such a way that the effect of low δ/D is, to some extent, similar to the effect of low q_0 in the uniformly stratified fluid of infinite extent (see figure 3 in Ermanyuk 2002).

Using (4.3), the total damping can be decomposed into wave and viscous components. The results of the decomposition for the data shown in figure 10 are presented in figure 11 in terms of the non-dimensional radiated wave power $C_p(\Omega)$. Note that at low Ω and small δ/D the experimental values of $C_p(\Omega)$ are systematically higher than the theoretical curve (solid line in figure 10) for a uniformly stratified fluid of infinite extent. In all the other cases studied in the present investigation (see figures 4 and 11 of Part 1 and figure 5 here), the theoretical curves for a uniformly stratified fluid of infinite extent give an upper estimate of $C_p(\Omega)$ for $0 < \Omega < 1$. This observation emphasizes the necessity of further theoretical investigations of dynamic interaction between oscillating bodies and a pycnocline, especially in the case $\delta/D = O(1)$.

4.3.2. Two-dimensional case

At this point it is pertinent to make some comments on the experimental curves $C_\lambda(\Omega)$ and $C_\mu(\Omega)$ presented in figures 3 and 5 of Part 1. In § 4.2.2. we have mentioned the importance of the low-frequency limit of the force coefficients. Indeed, since the damping coefficient in the two-dimensional problem is maximized when $\Omega \rightarrow 0$, the

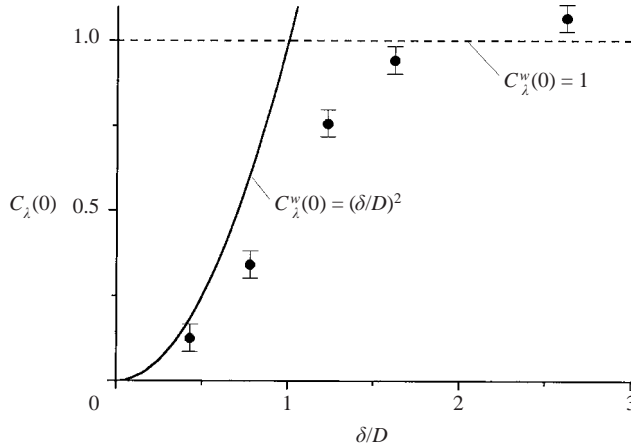


FIGURE 12. Low-frequency values of the non-dimensional damping coefficient $C_\lambda(0)$ of a cylinder in a pycnocline vs. non-dimensional pycnocline thickness δ/D . Points are taken from figure 6 of Part 1. Solid and dashed lines show the asymptotes for $\delta/D \ll 1$ and $\delta/D \gg 1$, respectively.

limiting value of $C_\lambda(0)$ is an important order-of-magnitude estimate. Recall that at $\Omega \rightarrow 0$ we can assume $C_\lambda \approx C_\lambda^w$. As discussed in §4.2.2, the low-frequency behaviour of $C_\lambda^w(\Omega)$ can be understood from a physical analogy with the blocking effect for uniform horizontal motion at low velocity. Obviously, when $\delta < D$ (more strictly, when $\delta \ll D$) the characteristic vertical extent of the blocked region is given by δ . For $\delta > D$ the blocked region has the vertical size D . Correspondingly, we can expect $C_\lambda^w(0) \sim (\delta/D)^2$ for $\delta < D$ and $C_\lambda^w(0) \approx 1$ for $\delta > D$. These functions are plotted in figure 12 together with experimental points taken from figure 6 of Part 1. Since the data at zero frequency could not be obtained, we took the available data on $C_\lambda(\Omega)$ at the lowest frequency as an experimental estimate for $C_\lambda(0)$. One can see that our simplistic considerations explain, at least qualitatively, the observed variation of the maximum damping with δ/D . It should be also noted that (4.4) is valid for the pycnocline stratification. Indeed, (4.4) follows from the assumption that $\mu_{11}(\omega) - i\lambda_{11}(\omega)/\omega$ has a simple pole at zero frequency. There are no apparent reasons to expect that any additional singularity may emerge in the case of pycnocline. Therefore, the general dependence of I on δ/D should be similar to that depicted in figure 12, i.e. we can expect that, asymptotically, $I \sim (\delta/D)^2$ for $\delta/D \ll 1$ and $I \approx \text{const}$ for $\delta/D \gg 1$. This conjecture is consistent with the data shown in figure 7 of Part 1. Numerical calculations performed in Motygin & Sturova (2002) for the limiting case $\delta/D \rightarrow 0$ (two-fluid system with an interface) agree well with the above conclusions. For a horizontally oscillating cylinder with its centre at the level of the undisturbed interface they show that $C_\mu \approx 1$ and C_λ is negligibly small for any frequency of oscillations.

5. Concluding remarks

In this work we have performed experiments with a sphere oscillating horizontally in a linearly stratified fluid of limited depth, and in a smooth pycnocline. The experimental technique used for evaluation of the force coefficients of the sphere is similar to the one used in the Part 1: the frequency-dependent added-mass and damping coefficients are evaluated from the Fourier-transforms of impulse response functions. It is shown that the three-dimensional case has some features that are different

from those observed in the two-dimensional case. For low-frequency oscillations the gravity effects are dominant and the flow of stratified fluid around the horizontally oscillating sphere is quasi-two-dimensional. Accordingly, the zero-frequency limit for the damping coefficient is $C_\lambda^w(0) = 0$ (merely a reflection of the D’Alambert paradox). If the vertical extent of stratification is greater than the vertical size of the sphere, then $C_\mu(0) = 1$, which is also true for any axisymmetric body with a vertical axis of rotation. In the two-dimensional case, the damping coefficient is maximized at zero frequency due to an effect similar to blocking that occurs for a body moving with uniform horizontal velocity in a stratified fluid.

The results presented in Part 1 and here suggest that, at least at first approximation, the total damping of two- and three-dimensional bodies oscillating in a continuously stratified fluid can be consistently decomposed into wave and viscous components using a version of Froude’s method. The viscous damping markedly increases as $H/D \rightarrow 1$, most notably in the two-dimensional case. The behaviour of the added-mass coefficient was found to be qualitatively and quantitatively consistent with the ideal-fluid concept, with weak manifestations of viscous effects at $H/D \rightarrow 1$.

It is found that the maximum mean power of internal waves radiated by a sphere oscillating in a linearly stratified fluid of limited depth and in a smooth pycnocline is reduced when the vertical extent of stratification decreases. The maximum of the frequency spectrum of wave power shifts toward lower frequency. Thus, the effect of the finite vertical extent of stratification on the radiated wave power is qualitatively similar in both the two- and three-dimensional cases. At the same time it is interesting to note that, for a sphere oscillating in the pycnocline, the radiated wave power C_p at low Ω can be greater than that predicted for a uniformly stratified fluid of infinite extent (see figure 11). In all the other cases studied in Part 1 (figures 4 and 11) and here (figure 5) the theoretical values of $C_p(\Omega)$ for a uniformly stratified fluid of infinite extent give an upper estimate of the radiated wave power for the whole frequency range $0 < \Omega < 1$.

In Part 1 we made an attempt to combine the results obtained in Gorodtsov & Teodorovich (1986) and Voisin (2003*b*) to evaluate the energy radiated with internal waves by a body oscillating in a uniformly stratified fluid of limited depth. It was shown that such an approach can capture, at least qualitatively, the main trend of experimental data obtained at different H/D . In the present paper, we have taken another look at the problem and discussed the experimental results in the context of the theory of affine similitude (Ermanyuk 2002). This approach generalizes the present results for the affinely similar experimental geometries.

The present experimental investigation is limited to the case of horizontal oscillations. For vertically oscillating bodies in a uniformly stratified fluid, functions $K_{33}^{(1)}(\Omega)$ can be obtained theoretically from (2.3) and (2.4). Hurley’s (1997) solution for a circular cylinder undergoing vertical oscillations in a uniformly stratified fluid of infinite extent should be mentioned. As discussed in Ermanyuk (2000), the results presented in Gavrilov & Ermanyuk (1997) confirm that the values of $K_{ij}^{(1)}$ for a circular cylinder do not depend on the direction of oscillations, in agreement with Hurley (1997) (the formal theoretical explanation is given in Hurley & Hood 2001). For the case of sphere, experiments with vertical damped oscillations have been performed by Larsen (1969). These experiments confirm his own time-domain analysis, which is equivalent to the frequency-domain analysis by Lai & Lee (1986) as discussed in Part 1. Recently, the problem considered by Larsen (1969) was revisited by Levitskii & Chashechkin (1999) with particular emphasis on the nonlinear effects and flow pattern. Processing of their data with the approach described in §3 demonstrated

good qualitative agreement with Lai & Lee (1986) or, equivalently, with expressions (2.3), (2.4) and (2.6) of the present paper.

This study was supported by the Russian Foundation for Basic Research under grant 0001-00812 and by Siberian Branch of Russian Academy of Sciences (SB RAS) under grant 6 for young scientists and grant 1-2000 of Integration Project SB RAS. The first author is grateful to the Science Support Foundation. The authors wish to thank Professor V. I. Bukreev and Professor I. V. Sturova for interesting discussions and Dr B. Voisin for stimulating scientific correspondence and discussions. Thanks are due to Dr V. A. Kostomakha for his technical help. The authors are grateful to the referees and the editor for their remarks which helped to improve the original manuscript.

REFERENCES

- BAINES, P. G. 1995 *Topographic Effects in Stratified Flows*. Cambridge University Press.
- BATCHELOR, G. K. 1967 *An Introduction to Fluid Dynamics*. Cambridge University Press.
- ERMANYUK, E. V. 2000 The use of impulse response functions for evaluation of added mass and damping coefficient of a circular cylinder oscillating in linearly stratified fluid. *Exps. Fluids* **28**, 152–159.
- ERMANYUK, E. V. 2002 The rule of affine similitude for the force coefficients of a body oscillating in a uniformly stratified fluid. *Exps. Fluids* **32**, 242–251.
- ERMANYUK, E. V. & GAVRILOV, N. V. 2002 Force on a body in a continuously stratified fluid. Part 1. Circular cylinder. *J. Fluid Mech.* **451**, 421–443.
- GAVRILOV, N. V. & ERMANYUK, E. V. 1997 Internal waves generated by circular translational motion of a cylinder in a linearly stratified fluid. *J. Appl. Mech. Tech. Phys.* **38**, 224–227.
- GORODTSOV, V. A. & TEODOROVICH, E. V. 1986 Energy characteristics of harmonic internal wave generators. *J. Appl. Mech. Tech. Phys.* **27**, 523–529.
- GUREVICH, M. I. 1940 Added mass of a lattice of rectangles. *Prikl. Mat. Mekh.* **4**, 523–529 (in Russian).
- HURLEY, D. G. 1972 A general method for solving steady-state internal gravity wave problems. *J. Fluid Mech.* **56**, 721–740.
- HURLEY, D. G. 1997 The generation of internal waves by vibrating elliptic cylinders. Part 1. Inviscid solution. *J. Fluid Mech.* **351**, 105–118.
- HURLEY, D. G. & HOOD, M. J. 2001 The generation of internal waves by vibrating elliptic cylinders. Part 3. Angular oscillations and comparison of theory with recent experimental observation. *J. Fluid Mech.* **433**, 61–75.
- IWATA, K. & MIZUTANI, N. 1987 Irregular wave forces acting on a submerged sphere. *Coastal Engng Japan* **30**, 117–130.
- IWATA, K., MIZUTANI, N. & KASAI, S. 1989 Wave forces acting on a submerged sphere under regular progressive waves. *Proc. JSCE* **405**, 215–224.
- KARANFILIAN, S. K. & KOTAS, T. J. 1978 Drag on a sphere in unsteady motion in a liquid at rest. *J. Fluid Mech.* **87**, 85–96.
- KOROTKIN, A. I. 1986 *Added Masses of a Ship*. Sudostroenie, Leningrad (in Russian).
- KOTIK, J. & MANGULIS, V. 1962 On the Kramers-Kronig relations for ship motions. *Intl Shipbuilding Prog.* **9**, 351–368.
- LAI, R. Y. S. & LEE, C.-M. 1981 Added mass of a spheroid oscillating in a linearly stratified fluid. *Intl J. Engng Sci.* **19**, 1411–1420.
- LANDAU, L. D. & LIFSHITZ, E. M. 1980 *Statistical Physics, Part 1*. Butterworth-Heinemann.
- LANDAU, L. D. & LIFSHITZ, E. M. 1987 *Fluid Mechanics*. Butterworth-Heinemann.
- LARSEN, L. H. 1969 Oscillations of a neutrally buoyant sphere in a stratified fluid. *Deep-Sea Res.* **16**, 587–603.
- LEVITSKII, V. V. & CHASHECHKIN, YU, D. 1999 Natural oscillations of a neutrally buoyant body in a continuously stratified fluid. *Fluid Dyn.* **34**, 641–651.
- MILNE-THOMSON, L. M. 1960 *Theoretical Hydrodynamics*. Macmillan.

- MOTYGIN, O. V. & STUROVA, I. V. 2002 Wave motions of a two-layer fluid driven by small oscillations of a cylinder intersecting the interface. *Fluid Dyn.* **37**, 600–613.
- NEWMAN, J. N. 1977 *Marine Hydrodynamics*. MIT Press.
- ODAR, F. & HAMILTON, W. S. 1964 Forces on a sphere accelerating in a viscous fluid. *J. Fluid Mech.* **18**, 302–314.
- SEDOV, L. I. 1965 *Two-dimensional Problems in Hydrodynamics and Aerodynamics*. John Wiley & Sons.
- STOKES, G. G. 1851 On the effect of the internal friction of fluids on the motion of pendulums. *Trans. Camb. Phil. Soc.* **9**, 8–106.
- STUROVA, I. V. 2001 Oscillations of a circular cylinder in a layer of linearly stratified fluid. *Fluid Dyn.* **36**, 478–488.
- TURNER, J. S. 1973 *Buoyancy Effects in Fluids*. Cambridge University Press.
- VLADIMIROV, V. A. & IL'IN, K. I. 1991 Slow motions of a solid in a continuously stratified fluid. *J. Appl. Mech. Tech. Phys.* **32**, 194–200.
- VOISIN, B. 2003a Oscillating bodies and added mass for internal gravity waves. Part 1. Spheres. *J. Fluid Mech.* (in preparation).
- VOISIN, B. 2003b Oscillating bodies and added mass for internal gravity waves. Part 2. Circular cylinders. *J. Fluid Mech.* (in preparation).
- WANG, C.-Y. 1968 On high-frequency oscillating viscous flows. *J. Fluid Mech.* **32**, 55–68.
- WEHAUSEN, J. V. 1971 The motion of floating bodies. *Annu. Rev. Fluid Mech.* **3**, 237–268.